# Predicting potential SNR gain for high field body imaging at 7 Tesla using radiative coil array element sensitivity patterns

**A. J. Raaijmakers[1], C. A. van den Berg[1], and D. W. Klomp[2]**
[1]Radiotherapy, UMC Utrecht, Utrecht, Netherlands, [2]Radiology, UMC Utrecht, Utrecht, Netherlands

## Introduction

Recent work has shown that for body imaging at high magnetic field strengths, MR coils have to be designed as far-field antennas to achieve maximum $B_1^+$ at larger depths. These antennas show considerable improvement both in transmit and receive properties in comparison to other designs [a]. However, image SNR is still not comparable to 3 T images. At high frequencies, the $B_1$ field attenuation by the human tissue is more severe. The question therefore arises whether the reduction in $B_1$-field penetration (and thereby reduced sensitivity of the coils) is not canceling all the potential gain in SNR of imaging at 7 Tesla. Ocali and Atalar[b] have shown that for a hypothetical ultimate coil array, the increase in SNR at 7 Tesla should be significant. However, this is done by comparing hypothetical $B_1$-field distributions that are constructed by an infinite series of plane wave basis functions. In this work, we will investigate more realistic coil sensitivity patterns and their SNR distributions and how they relate to magnetic field strength and depth inside the body.

$$V_{signal} \sim \rho \frac{B_1^-}{I} \omega \qquad V_{noise} \sim \sqrt{4kTBWR} \sim \sqrt{R}$$

$\rho$: *spin density*
$\frac{B_1^-}{I}$: *receive field per unit current*
k: *Boltzman constant*
T: *Temperature*
BW: *Bandwidth*
R: *Impedance of coil*

$$\rightarrow SNR \sim \frac{\rho\omega}{\sqrt{R}} \frac{B_1^-}{I} \sim \omega^2 \frac{B_1^-}{\sqrt{P}} \qquad [1]$$

## Materials & methods

The SNR was calculated from equation [1]. Note that simulated $B_1^-$ distributions that are normalized to 1 W input power show the spatial SNR distribution that is, in this study, defined as the coil sensitivity. Two realistic coil array elements are characterized by FDTD simulations (SEMCAD, SPEAG, Zurich, CH) at 1.5 T (64 MHz), 3 T (128 MHz), 7 T (298 MHz), 9.4 T (400 MHz) and 11.7 T (500 MHz). These are a 10 cm diameter loop coil and a single-side adapted dipole antenna (radiative antenna). These elements have demonstrated large signal penetration at 298 MHz [a]. The radiative antenna at 298 MHz has a 7 x 4.2 x 14.3 $cm^3$ substrate with a permittivity of 36. The legs of the dipole antenna are 10 x 5.3 $cm^2$ perfect conductors. These dimensions scale inversely with the frequency to ensure a $\lambda/2$ standing wave over the dipole antenna legs. The phantom is a 100 x 100 x 60 $cm^3$ phantom with a permittivity of 36 and a conductivity of 0.45. These values are averages between the dominant tissue types in the pelvis: fat and muscle. Both tissue types vary little over the investigated frequency range so the dielectric phantom properties were considered constant in this analysis. For the array simulations, eight elements were placed around an ellipsoid phantom (40 and 20 cm diameter) with the same material properties.

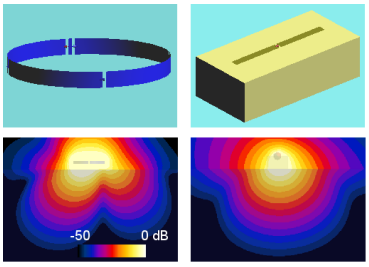


*Figure 1: Simulation geometries of coil elements: (a) loop (b) radiative antenna, and $B_1^-$ distributions at 7 T: (c) loop (d) radiative antenna*

## Results

Realistic $B_1^-$ field distributions were simulated for a loop coil and a radiative antenna. Sensitivity distributions are presented in figure 1. In-depth coil sensitivity profiles for the investigated magnetic field strengths are presented in figure 2a and b. From these results can be derived

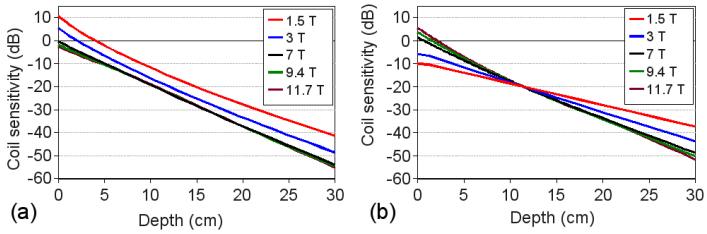


*Figure 2: Coil sensitivities or $B_1^-$ per unit power for various magnetic field strengths as a function of depth in the phantom. (a) loop coil (b) radiative antenna*

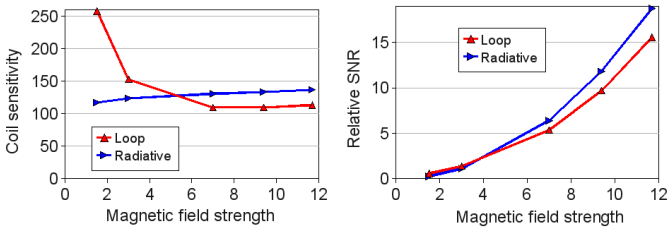


*Figure 3: Coil sensitivities and subsequent relative SNR at 10 cm depth for loop coil and radiative antenna as a function of magnetic field strength ($B_0$)*

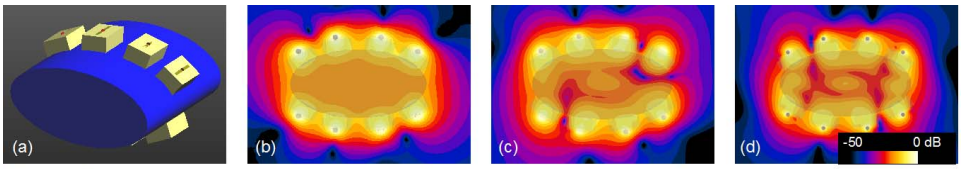


*Figure 5: Phase-shimmed sensitivity distributions for coil array of radiative antennas on ellipsoid phantom (a) setup (b) 3 T (c) 7 T (d) 9.4 T. Note that center of phantom shows sum-of-magnitude values and these are equal for all $B_0$-field strengths.*

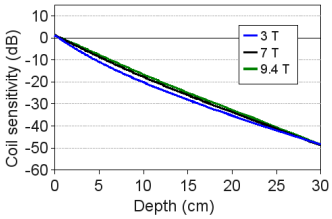


*Figure 4: Coil sensitivities at 3, 7 and 9.4 T for a radiative antenna with constant dimensions (tuned by inductors).*

that for realistic coil array elements, the coil sensitivity as a function of $B_0$-field strength becomes constant beyond 6 Tesla (figure 3). As a result, the SNR gain goes quadratic with $B_0$-field from this point until at least 11.7 Tesla (figure 3). Note that the loop coil sensitivity is considerably higher for 1.5 and 3 Tesla (figure 2a). A loop coil has (almost by definition) a strong inductive near-field. At the lower $B_1$ frequencies of 1.5 and 3 Tesla, the near-field penetrates into the phantom which results in higher $B_1$ levels. Almost all coils in MR imaging rely on this principle. At higher magnetic field strengths and deeply located target regions, coils have to rely on their far-field. The far-field sensitivity of the loop coil apparently does not depend much on the frequency (for $\sigma$=0.45 and up to a depth of 30 cm). This does not seem to apply for the radiative antenna: the slopes of the profiles decrease heavily with $B_0$-field strength (figure 2b). This is caused by the decreasing antenna dimensions with frequency. Therefore, with increasing frequency the aperture of the antenna decreases which results in a steeper slope of the logarithmic sensitivity profiles (figure 2b). Figure 4 shows sensitivity profiles where the dimensions of the radiative antenna are kept constant and tuning is done by inductors at either side of the feeding point. Now the radiative antenna shows the same far-field behavior as the loop coil: the coil sensitivity at depth is independent of frequency. This kind of tuning was also used in the array simulations that are presented in figure 5. These results show that also when combining radiative antennas into an array, the sensitivity does not change much with B1 frequency for far-field antennas.

## Conclusion

These results show that the SNR for body imaging at 7 Tesla is expected to become higher than the SNR at lower magnetic field strengths. Additionally, the increase in SNR with magnetic field strength should continue for any magnetic field strength that is now feasible for human imaging.

References:
[a] Raaijmakers et al. "Prostate Imaging at 7T..." ISMRM 2010 proceedings
[b] Ocali et al. MRM 39:462-47